16th World Conference on Earthquake, 16WCEE 2017

Santiago Chile, January 9th to 13th 2017

Paper N° 3484

Registration Code: S-B1460541825

CYCLIC RESPONSE OF AN ANTISEISMIC STEEL DEVICE FOR BUILDINGS-AN EXPERIMENTAL AND NUMERICAL STUDY

M.D. Titirla[(1)], P.K. Papadopoulos[(2)], I.N. Doudoumis[(3)] and K.V. Katakalos[(4)]

[(1)] *Civil Engineer, MSc, Phd student, Aristotle University of Thessaloniki, mtitirla@civil.auth.gr*
[(2)] *Assistant Professor, Aristotle University of Thessaloniki, paniko@civil.auth.gr*
[(3)] *Professor, Aristotle University of Thessaloniki, doud@civil.auth.gr*
[(4)] *Dr, Aristotle University of Thessaloniki, kkatakal@civil.auth.gr*

Abstract

The present study is focusing on the experimental and numerical evaluation of the effectiveness of an anti-seismic steel device. The developed device, mentioned as CAR1, belongs to the passive energy dissipation systems, as it does not require external power to generate system control forces. It can be used on new or existing structures and can be easily adapted to the particular demands of these. It can be installed in a variety of configurations such as in single or X diagonal bracing in building frames. Moreover the use of this device may result in improving (i) the increase of stiffness, (ii) the absorption of seismic energy, (iii) as well as a control of the axial forces that are developed in the diagonal steel braces. The main part of CAR1 is the groups of superimposed blades, which absorb seismic energy through simultaneous friction and yield. The number and the dimensions of these blades, their elastoplastic properties as well as the friction coefficient over their interface, define the equivalent nonlinear constitutive law of the diagonal bars as a function of their axial force. A Full scale CAR1 device was experimentally investigated under cyclic loading. The experimental load cases were conducted at the Laboratory of Experimental Strength of Materials and Structures of Aristotle University of Thessaloniki. The experimental sets are based on the investigation of the thickness, the cross-section and material of the blades, under different scenarios of cyclic loading with either constant or increasing load. In addition, as far as the numerical study is concerned, Finite Element Models of CAR1 device were developed and analyzed using ABAQUS software, thereby evaluating the reliable performance of the device. In order to simulate the behaviour of the group of the blades in ABAQUS, an explicit dynamic analysis was chosen, on the basis that this type of analysis allows for the definition of - general contact conditions encountered in complicated contact problems, without generating numerical difficulties. After completion of the experiments, the numerical results were compared with the respective experimental ones. Good agreement was shown and further useful results were observed.

Keywords: *Experimental validation; FEM; Absorption Seismic Energy; Passive Energy Dissipation System.*

1. Introduction

The safety of constructions (existing or new) is one of the major priorities of engineering globally, because structures are likely to be subjected to large and often devastating, for their integrity, loadings. Therefore, great interest arises to the study of innovations upon the design and materials of construction that minimize the probability of structural failure to a great range of loading. This is why many efforts have been made to create devices that are able to absorb the majority of the seismic energy but do not belong to the bearing structure. The main advantage of these is the easy replacement or repair. These devices belong to the category of passive energy dissipation systems; they do not require external power to generate system control forces and hence, are easy and cheap to be implemented on a structure.

Passive energy dissipation devices such as visco-elastic dampers, metallic dampers and friction dampers have been widely used to reduce the dynamic response of civil engineering structures subjected to seismic loads [1, 2, 3, 4]. Their effectiveness with regard to the seismic design of building structures is attributed to minimal structural damages, through absorption of the structural vibrational energy and dissipation via their inherent hysteretic behavior. So, several of these devices have been selected for seismic strengthening of existing or new buildings in the USA, Canada and Japan [5, 6, 7, 8, 9].

In order to demonstrate the effectiveness of the devices, many passive energy dissipation systems were studied under either experimental research [10, 11, 12, 13] or numerical research [14, 15, 16]. Considering the numerical research developed on the passive energy dissipation devices, two different approaches have been followed: (i) the macromodels, based on the physical understanding of each device, and (ii) the micromodels, based on a finite element (FE) representation of each device. FE models play a key-role in the ordinary design process of new structures and in the assessment of existing ones [17]. The Finite Element Method (FEM) has become the most popular method in both research and industrial numerical simulations, as it takes into consideration material laws, contact interface conditions and others parameters, which lead to the exact response of the device. Several algorithms, with different computational costs, are implemented in the finite elements codes, such as ABAQUS [18], which is a commonly used software for finite element analysis. Comparison between the numerical results and the respective experimental ones, is very useful and necessary as it provides the opportunity to researchers to study the behavior of their devices more in breadth [19, 20, 21]. The calibrated FEM models are used to conduct a series of simulations to study the effect of different parameters. In this way, results come out which would otherwise be hard to obtain experimentally.

In this present paper, a novel anti-seismic steel device (with code name CAR1) for seismic strengthening of existing or new buildings, which was recently developed at the Laboratory of Experimental Strength of Materials and Structures of Aristotle University of Thessaloniki, is studied experimentally. Its effectiveness has been numerically verified [22, 23]. The aim of the present study is to numerically replicate the experimentally obtained results in order to create a reliable tool for the simulation of the hysteretic behavior of the device CAR1 so as to identify the key parameters controlling the response of the CAR1 device .

2. Description of the investigated device CAR1

The developed device has the codename CAR1 and belongs to the passive energy dissipation system, as it does not require external power to generate system control forces. This device is proposed by Papadopoulos et al. [22] and it consists of 4 main elements, as illustrated in Fig. 1. The exterior tube, the interior shaft, five groups of superimposed blades and the restraint bolt. The relevant movement between the exterior tube (Element A) and the interior shaft (Element B) is undertaken by an elastoplastic bending deformation of the superimposed blades that connect cross-wise elements A and B. The number and the dimensions of the superimposed blades as well as their elastoplastic properties govern the elastoplastic behavior of the diagonal bars under an axial load. There is also provision for a Restraint bolt (stoppage bolt). This bolt is made of high yield Steel, and can slide inactively through an appropriately selected oval hole at Element B. As a result, the activation of this bolt takes place at a “second time” and enables the desired plastic deformations of the superimposed steel blades to happen. The activation of the stoppage bolt allows the transfer of an additional axial load from elements A to element B of the device. An appropriate configuration / geometry in the area of the stoppage bolt (oval hole) eliminates any additional compression forces on the diagonal elements and allows only tensional forces to be developed.

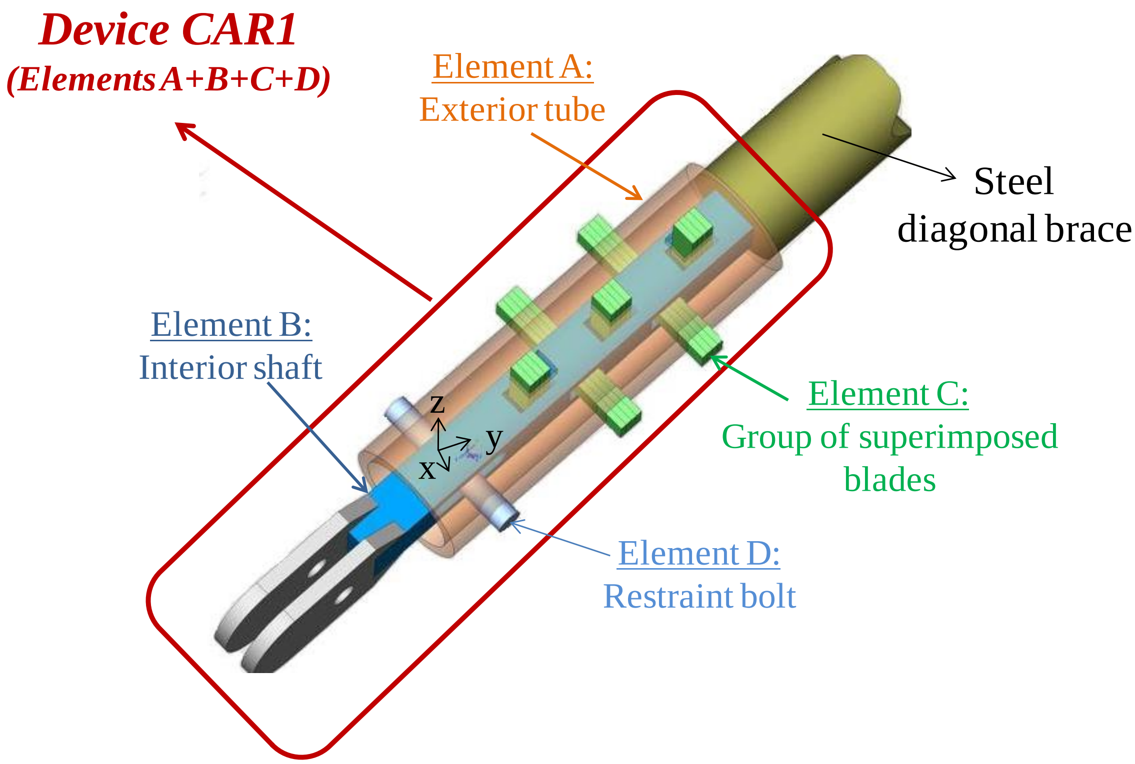

Fig. 1 – The investigated device CAR1.

Device CAR1 has the advantage to (i) provide additional stiffness as well as, (ii) absorption of seismic energy, through yield and friction, (iii) provision for control of the axial forces that are developed at the diagonal steel rods and last but not least the ability to retain the plastic displacements up to a desired level, due to the restraint bolt. Energy dissipation is provided by the inelastic bending of the superimposed blades.

The device CAR1 can be used in new or existing structures and can be easily adapted to the particular demands of each structure-. However, it can be installed in a variety of ways which include arranging them in single diagonal braces or in X braces (Fig. 2) and in accordance with the requirements of each structure, one or more such devices can be used.

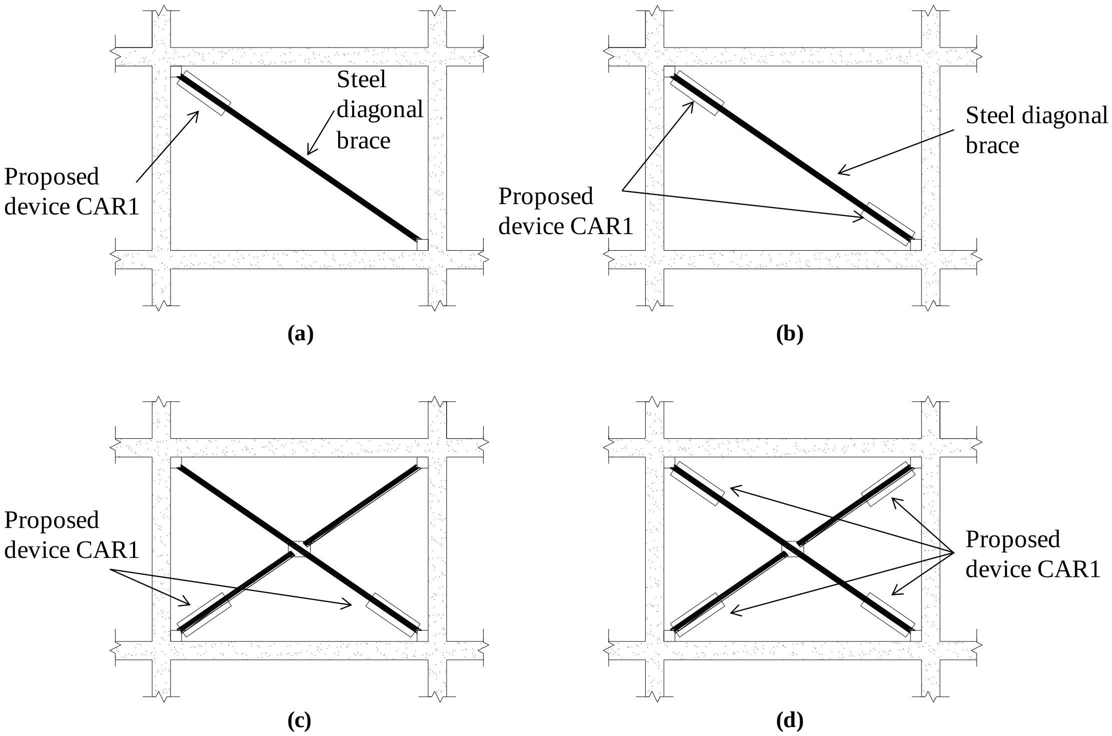

Fig. 2 - The possible position of the device CAR1, incorporated into steel diagonal braces.

3. Experimental Investigation

A Full scale CAR1 device was experimentally investigated under cyclic loading. The experimental load cases were conducted at the Laboratory of Experimental Strength of Materials and Structures of Aristotle University of Thessaloniki. The specimen details of the experiment are depicted in Fig. 3. The load was controlled with a 100kN capacity load cell under displacement control. Two Linear Variable Differential Transformers (LVDT) were positioned at each side of the longitudinal axis of the device CAR1, which measure the relative movement of the interior shaft to the exterior tube. All data was recorded and stored in a digital data system via a computer. We can notice from Fig. 3 that only two group of superimposed blades were tested. Every group consists of five steel blades, each 4mm thick.

A standard test has been carried out in order to establish the basic material properties of the superimposed blades. These experimentally derived material properties were utilized in the subsequent numerical study. The grade of the steel of the blades was S235. The experimentally derived Young's modulus E, Yield Stress σ_y and maximum Stress σ_u are reported in Table 1.

Table 1 - Material properties of steel blades.

Material	Young Modulus E (Gpa)	Yield Stress σ_y (Mpa)	Maximum Stress σ_u (MPa)
Steel	203.6	220	290

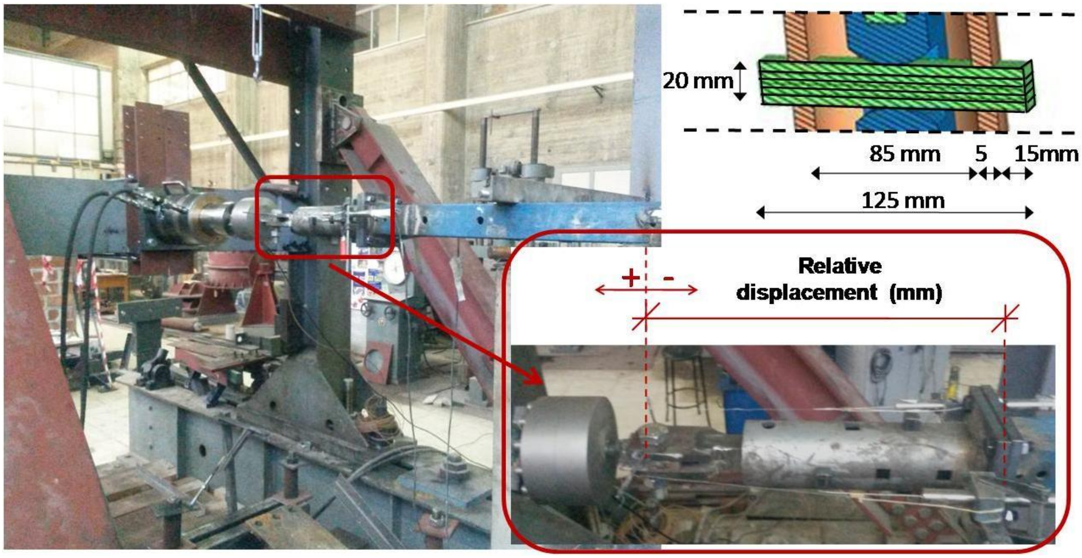

Fig. 3 - Experimental Setup.

Quasi-static cyclic tests were carried out in order to ascertain the behavior of the CAR1 device toward the absorbed seismic energy. Two sequences have been conducted. First sequence is one cycle with target load equal to 75kN with a rate of 18kN/minute equivalent to relevant displacements 14mm, while second sequence is 17 cycles displacement control with values starting from 4.5 mm up to 10 mm with a rate of 3mm/minute.

Fig. 4 shows the hysteresis loops that emerged from the experimental sequences. The First sequence is indicated with a red line, while the second with a blue line. The area within a hysteresis loop is equivalent to the amount of seismic energy that the device is dissipating. It is observed that the shape and consistency of the hysteresis loops remain constant during the repeated cycles, which proves that the device CAR1 is effective to dissipate seismic energy whereas it will not break during the repeated cycle loading.

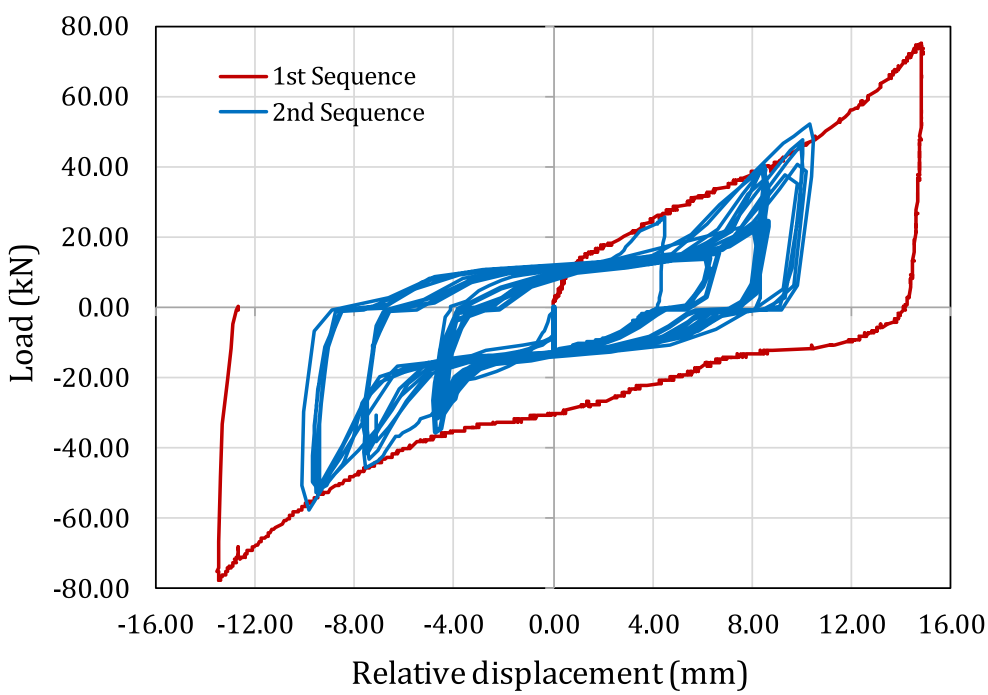

Fig.4 - Experimental hysteresis loops.

4. Finite Element Simulation

The general purpose FE software ABAQUS was employed to generate FE models in order to numerically simulate the behavior of the CAR1 device. An explicit dynamic solver was selected to allow for the definition of general contact conditions encountered in complicated contact problems, without generating numerical difficulties. The explicit dynamic analysis procedure is based upon the implementation of an explicit integration rule together with the use of diagonal ("lumped") element mass matrices.

The explicit dynamic FEA analysis of braced frame systems under quasi-static loading may become affected with a number of potential complications. Specifically, the structure may suddenly gain inertia, which can cause not real-life oscillations, if the analysis completion time is not carefully adjusted. Therefore, in order to achieve, in the finite element analysis, real life quasi-static responses, the loads must be applied slowly. Upon achieving accurate quasi-static results, the kinetic energy of the simulated models shall remain low. The general available recommendation [18] is to keep the kinetic energy lower than 10% of the internal energy throughout the simulation. However, the current study will show that a lower threshold (i.e., less than 2%) has to be achieved, because blades buckling may initiate not real-life dynamic oscillations.

The FEM model geometry reproduced the actual geometry of the tests set-up of the CAR1 device. Fig. 5 shows the FEM model together with its boundary conditions. The superimposed blades are free to move along the axis x-x, independent of each other. The movements along the axis y-y and z-z are prohibited because of the existence of the external tube (Element A). The definition of the boundary conditions for the superimposed blades is not considered necessary as these are simply mounted onto the rigid components of the exterior tube A of the device . On the other hand, exterior tube is fixed (all degrees of freedom) while interior shaft is free to move only in z-z axis. The geometry of the FE model was reproduced in full detail.

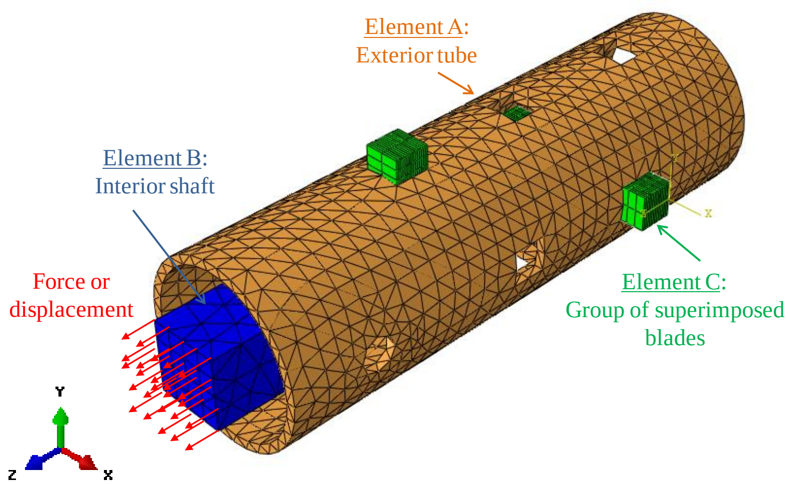

Fig. 5 - The FEM model used for the device CAR1.

Several simulations were conducted to identify the best meshing. For the explicit method, blades and interior shaft are meshed using 3D reduced integration solid element **C3D8R** (eight-node bricks), while exterior tube is meshed using 3D solid element **C3D4** (four-node tetrahedron) available in ABAQUS. Normally, a higher mesh density provides for higher accuracy but also increases the computational time without improving substantially the accuracy of the results, therefore, a trade-off between time and accuracy becomes crucial [25]. The final mesh has 8126 elements and the result was a solution that correlated with the experimental results.

The uniaxial stress–strain corrrelation of the blades, exterior tube and interior shaft are modeled as elastic with Young's modulus (Es) and Poisson's ratio (v) at typical values of 200 GPa and 0.3, respectively. Plastic behavior is defined in a tabular form, including yield stress and corresponding plastic strain. The experimentally obtained stress (σ_{nom})-strain (ε_{nom}) curves for the blades was converted into the true stress (or Cauchy) (σ_{true})-

logarithic plastic strain ($\varepsilon_{\ln}^{pl}$) format according to Eq. (1) and (2) and was further utilized in order to define the material response.

$$\sigma_{true} = \sigma_{eng}\left(1 + \varepsilon_{eng}\right) \tag{1}$$

$$\varepsilon_{pl} = \varepsilon_{true} - \frac{\sigma_{true}}{E} \tag{2}$$

Surfaces in contact are not only the interior surfaces of the superimposed steel blades, but also a part of the exterior tube with the interior shaft, upon which the blades sit. The surface-to-surface contact formulation technique with small sliding between the contacting surfaces was chosen. The contact definition includes the specification of two surfaces, one acting as the ‘‘master’’ surface and the other as the ‘‘slave’’ surface. The contact algorithm searches whether the nodes of the slave surface are in contact with the nodes of the master surface and enforces contact conditions in an average sense over a region of slave nodes using a Lagrange multiplier formulation [18]. A friction coefficient equal to 0.2 [25] was assumed between the contacting surfaces.

Quasi-static response was achieved by specifying a slow displacement rate and checking that the kinetic energy was smaller than 2% of the internal energy for the greatest part of the analysis. The load/displacement was imposed upon the interior shaft and transferred to the center of the superimposed blades. The imposed displacement/load history was based on the experimental sequences.

5. Results and Discussion

Fig. 6 plots - Force versus Relevant Displacement by the FEM analyses along with the experimental hysteresis of the two sequences. Blue lines illustrate hysteresis loops of experiments, while green lines show hysteresis loops of the Finite Element Models. The FEM predicted values for the load and displacement are in very good agreement with the corresponding experimental ones. The comparisons between the FEM analyses and the experiments show that the proposed FEM model is capable of reproducing the inelastic response of the CAR1 device. Therefore, it is a reliable tool for the simulation of the hysteretic behavior of the CAR1 device and can be used in further studies in order to investigate the effect of various parameters.

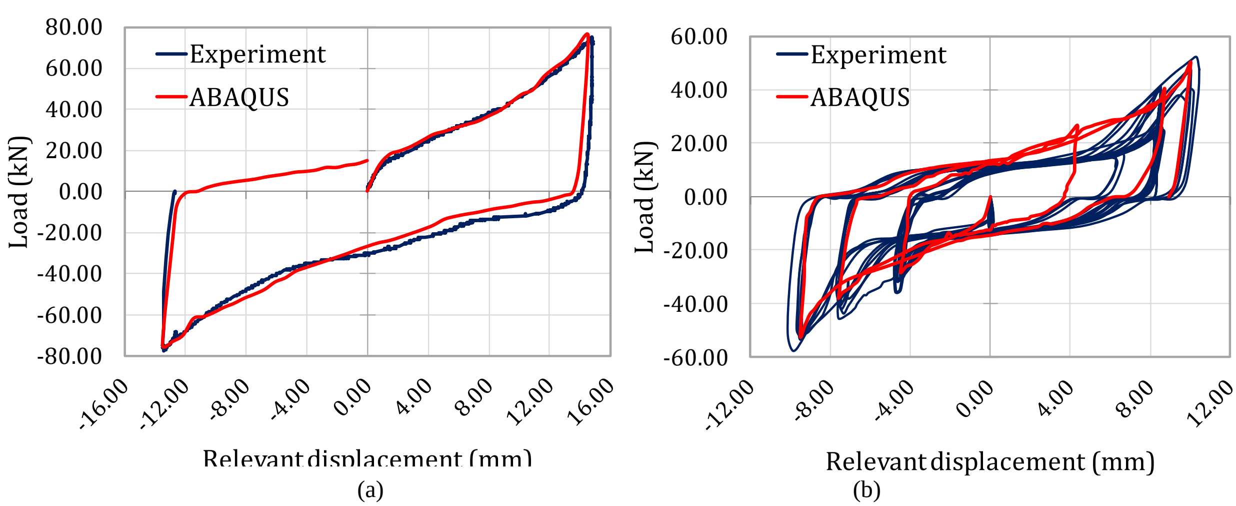

Fig. 6 - Comparison of the experimental and the numerical force–displacement hysteresis of the device CAR1 (a) 1st Sequence, (b) 2nd Sequence.

Fig. 7 shows the distribution of the contact stresses on the surfaces of the blades (top view of the 1st and 3rd blade and bottom view of the 5th blade) during the cycle of the 1st Sequence, while Fig. 8 illustrates the distribution of the Von Misses stress. It can be observed that the maximum pressures develop in the bottom view of the 5th blade, at the contact surfaces with the exterior tube, for relevant movement Uz=14.00mm and in the top view of the first blade, at the region where there is contact with the exterior tube, for a relevant movement of Uz=-14.00mm. In addition, upon reset of the device at the relevant displacement of Uz=0.00mm, small pressures develop at the group of the superimposed blades because of the permanent deformation.

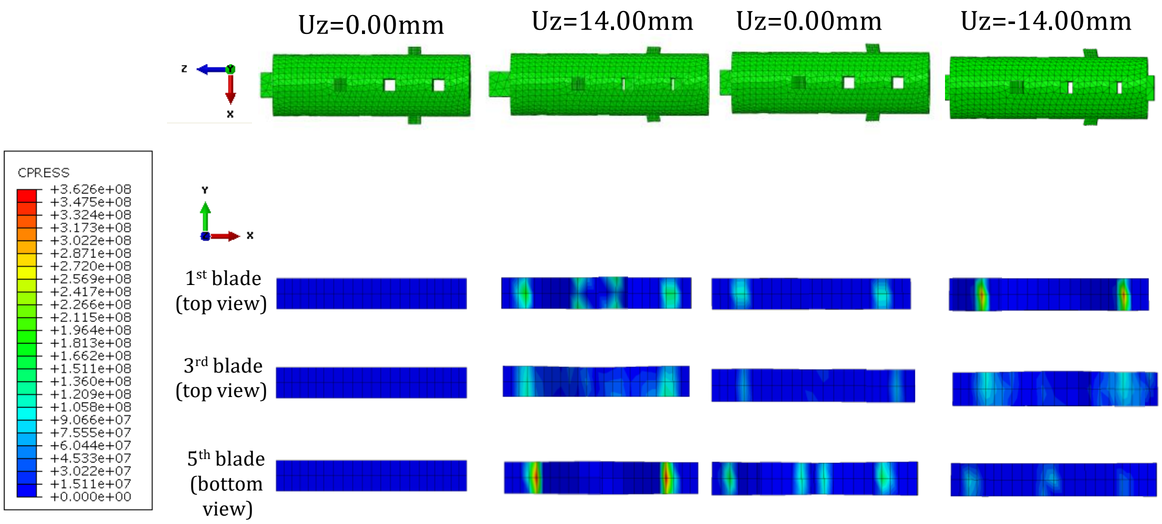

Fig. 7 - Distribution of contact stresses on surfaces of blades (top view of 1st and 3rd blade and bottom view of 5th blade) during the cycle of the 1st Sequence (values in Pa).

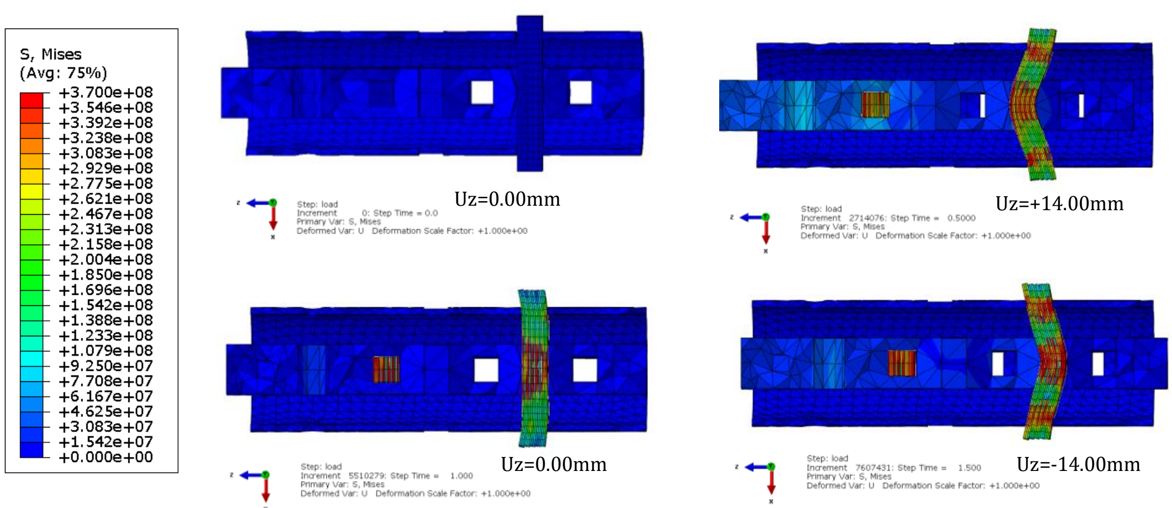

Fig. 8 - Stress distribution in device CAR1 based on Von Misses Criteria (values in Pa).

The numerical deformed shapes are compared with the corresponding experimental ones for relevant movements of Uz=+5mm and Uz=-5mm, as in Fig. 9. During the bending of the superimposed blades, the first blade slides against the second blade, etc, resulting to frictional forces being developed.

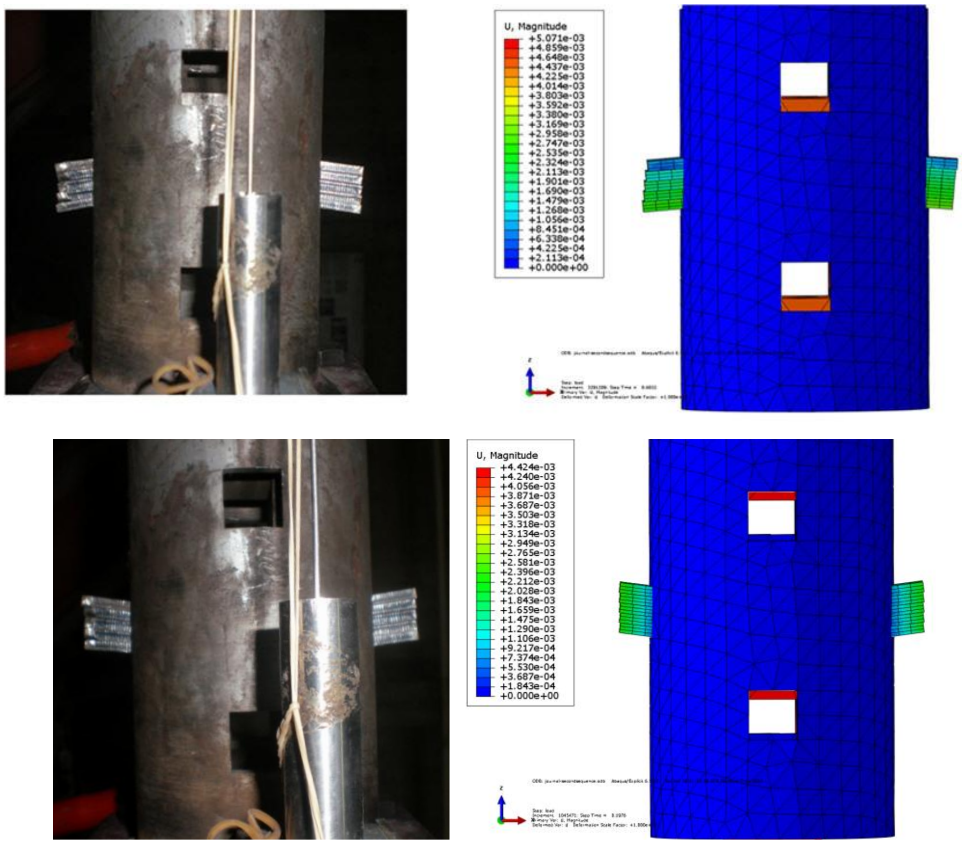

Fig. 9 - Distribution of deformed shapes (values in m).

6. Conclusions

In this present study, a novel anti-seismic steel device (CAR1) for the seismic upgrade of existing or new buildings, which was recently developed at the Laboratory of Experimental Strength of Materials and Structures of Aristotle University of Thessaloniki, is experimentally studied. An advanced non-linear finite element model (FEM) was also developed. This model was calibrated against experimental results and further used to shed light on the response of the device CAR1.

Based on the findings of the present investigation, the following conclusions are drawn:

1. Device CAR1 is a reliable energy dissipation device, which can be used in new or existing structures and minimize the probability of structural failure against almost any external load.
2. The developed non-linear FEM models can be reliably used to assess the behaviour of the proposed anti-seismic steel device CAR1, since they are capable to track down the hysteretic behavior and predict the deformed shape of the device with good accuracy.
3. Based on the shape and consistency of the hysteresis loops, these will remain constant under the repeated cyclic load whereas the device will not break. The device CAR1 dissipated energy due to (i) the plastic strain of the superimposed blades during the cyclic and (ii) the friction forces. The amount of dissipated energy is higher when the friction exists and with the coefficient of friction carrying the maximum value, leading to to double the total energy dissipated, compared to the frictionless system.

4. What is more, the calibrated (E, σ_y, σ_u) FEM model permits an in-depth investigation of the stress state in the blades and helps to identify all possible local failures

7. Acknowledgements

The authors would like to sincerely thank the staff of the Laboratory of Experimental Strength of Materials and Structures of Aristotle University of Thessaloniki for their help. Also, the authors would like to thank Alkis Papadopoulos, PhD Candidate at Aristotle University of Thessaloniki, for his support provided during the experiments.

8. References

[1] Aiken ID, Nims DK & Kelly JM (1992): Comparative study of four passive energy dissipation systems. *Bulletin of the New Zealand National Society for Earthquake Engineering*, **25**(3), 175-192.

[2] Constantinou CM, Symans MD, Taylor DP (1993): Fluid viscous damper for improving the earthquake resistance of buildings. *Structural Engineering in Natural Hazards Mitigation*, 718-723.

[3] Soong T, Spencer JrBF (2002): Supplemental energy dissipation: state-of-the-art and state-of-the- practice. *Engineering Structures*, **24**, 243-259.

[4] Symans MD, Charney FA, Whittaker AS, Constantinou MC, Kircher CA, Johnson MW, McNamara RJ (2008): Energy dissipation systems for seismic applications: Current practice and recent developments. *Journal of Structural Engineering*, **134** (1), 3-21.

[5] Pall AS, Verganelakis V, March C (1987): Friction-Dampers for seismic control of Concordia University Library Building. *Proc 5th Canadian Conference on Earthquake Engineering*, Ottawa, USA.

[6] Keel CJ, Mahmoodi P (1986): Designing of Viscoelastic Dampers for Columbia Center Building. *Building Motion in Wind, (N. Isyumov and T. Tschanz, Editors), ASCE*, NY, 66-82.

[7] Makris N, Constantinou MC (1992): Spring-Viscous Damper Systems for Combined Seismic and Vibration Isolation. *Earthquake Engineering and Structural Dynamics*, **21**, 649-664.

[8] Martinez-Romero E (1993): Experiences on the Use of Supplemental Energy Dissipators on Building Structures. *Earthquake Spectra*, **9**(3), 581-624.

[9] Pasquin C, Pall A, Pall R (1994): High-Tech Seismic Rehabilitation of Casino de Montreal, *Structures Congress*, Atlanta, Georgia, **2**, pp. 1292- 1297.

[10] Whittaker AS, Bertero VV, Alonso JL, Thompson CL (1989): Earthquake Simulator Testing of Steel Plate Added Damping and Stiffness Elements. *Report No. UCB/EERC 89/02*, University of California, Berkley.

[11] Anagnostides G, Hargreaves AC, Wyatt TA (1989): Development and applications of energy absortion devices based on friction. *J. Construct. Steel Research*, **13**, 317-336.

[12] Aiken ID, Nims DK, Whittaker AS, Kelly JM (1993): Testing of passive energy dissipation systems. *Earthquake Spectra*, **9**(3), 335-370.

[13] Papadopoulos PK, Salonikios Th, Dimitrakis S, Papadopoulos A (2013): Experimental investigation of a new steel friction device with link element foe seismic strengthening of structures. *Structural Engineering & Mechanics*, **46**(4).

[14] Pall AS, March C (1982): Seismic response of friction damped braced frames. *ASCE, Journal of Structural Division*, **108** (9), 1313-1323.

[15] Papadopoulos P (2012): New nonlinear anti-seismic steel device for the increasing the seismic capacity of multi-storey reinforced concrete frames. *The structural design of tall and special buildings*, **21**, 750-763.

[16] Ramirez JDM, Tirca L (2012): Numerical Simulation and Design of Friction- Damped Steel Frame Structures damped. *15th World Conference in Earthquake Engineering*, Lisboan, Portugal.

[17] Brownjohn JMW, Xia PQ, Hao H, Xia Y (2001): Civil structure condition assessment by FE model updating: methodology and case studies. *Finite Elements in Analysis and Design*, **37**(10), 761-775.

[18] Abaqus Simulia, (2012). Analysis User's Manual Volume IV. Analysis User's Manual Volume IV . Providence: Dassault Systèmes.

[19] Stefancu AI, Budescu M, Paulet-CrainiceanunF, Guerreiro LMC (2012): Numerical and experimental analysis of a passive multilayer friction damper for seismic energy dissipation. *15th World Conference on Earthquake Engineering*, Lisboan, Portugal.

[20] Vasdravellis G, Karavasilis Th, Uy Br (2013): Finite element models and cyclic behavior of self-centering steel post-tensioned connections with web hourglass pins. *Engineering Structures*, **52**, 1-16.

[21] Manos G.C, Theofanous M, Katakalos K (2014): Numerical simulation of the shear behaviour of reinforced concrete rectangular beam specimens with or without FRP-strip shear reinforcement. *Advances in Engineering Software,* **67**, 47-56.

[22] Papadopoulos PK, Titirla MD, Papadopoulos AP (2014): A new seismic energy absorption device through simultaneously yield and friction used for the protection of structures. *2nd European Conference on Earthquake Engineering and Seismology*, Istanbul.

[23] Titirla MD, Papadopoulos PK, (2015): Finite element investigation of a new seismic energy absorption device through simultaneously yield and friction. *5th ECCOMAS Thematic Conference on Computational Methods in Structural Dynamics and Earthquake Engineering*, Crete; Greece, 4065-4077

[24] Doudoumis IN (2007): Finite element modelling and investigation of the behaviour of elastic infilled frames under monotonic loading. *Engineering Structures*, **29**, 1004–1024.

[25] Eurocode 3, (2003). Design of steel structures. Part 1-8: design of joints. prEN 1993-1-8:2003. European Committee for standardization: Brussels.